AD-A057 359   CHARLES STARK DRAPER LAB INC CAMBRIDGE MA   F/G 4/1
               STUDY OF RADIATIVE TRANSFER IN SCATTERING ATMOSPHERES.(U)
               JUN 77   C K WHITNEY, H L MALCHOW   F19628-76-C-0223
UNCLASSIFIED   R-1092   AFGL-TR-78-0101   NL

| OF |
AD
A057 359

END
DATE
FILMED
9-78
DDC

LEVEL II

(4)

AD A057359

(18) (19)
AFGL-TR-78-0101

(6)
STUDY OF RADIATIVE TRANSFER
IN SCATTERING ATMOSPHERES.

Cynthia K. Whitney
Harvey L. Malchow

The Charles Stark Draper Laboratory, Inc.
555 Technology Square
Cambridge, Massachusetts 02139

(13) 24 p.

(11) June 77

(14) R-1092

(9)
Final Report
1 June 76 — 30 May 1977,

(15) F19628-76-C-0223

(16) 7621

(17) 14

Approved for public release; distribution unlimited

AIR FORCE GEOPHYSICS LABORATORY
AIR FORCE SYSTEMS COMMAND
UNITED STATES AIR FORCE
HANSCOM AFB, MASSACHUSETTS 01731

78 08 03 29

408 386

Qualified requestors may obtain additional copies from the Defense
Documentation Center. All others should apply to the National
Technical Information Service.

LEVEL II ④

REPORT DOCUMENTATION PAGE

READ INSTRUCTIONS
BEFORE COMPLETING FORM

1. REPORT NUMBER AFGL-TR-78-0101	2. GOVT ACCESSION NO.	3. RECIPIENT'S CATALOG NUMBER
4. TITLE (and Subtitle) STUDY OF RADIATIVE TRANSFER IN SCATTERING ATMOSPHERES		5. TYPE OF REPORT & PERIOD COVERED Final Report (1 June 76 to 30 May 77)
		6. PERFORMING ORG. REPORT NUMBER R-1092
7. AUTHOR(s) Cynthia K. Whitney, Harvey L. Malchow		8. CONTRACT OR GRANT NUMBER(s) F19628-76-C-0223
9. PERFORMING ORGANIZATION NAME AND ADDRESS The Charles Stark Draper Laboratory, Inc. Cambridge, Massachusetts 02139		10. PROGRAM ELEMENT, PROJECT, TASK AREA & WORK UNIT NUMBERS 62101F 762114AA
11. CONTROLLING OFFICE NAME AND ADDRESS Air Force Geophysics Laboratory, Inc. Hanscom AFB, Massachusetts 01731 Monitor/Eric Shettle/OPA		12. REPORT DATE June 1977
		13. NUMBER OF PAGES 36
14. MONITORING AGENCY NAME & ADDRESS (if different from Controlling Office)		15. SECURITY CLASS. (of this report) Unclassified
		15a. DECLASSIFICATION/DOWNGRADING SCHEDULE

16. DISTRIBUTION STATEMENT (of this Report)

Approved for public release; distribution unlimited.

17. DISTRIBUTION STATEMENT (of the abstract entered in Block 20, if different from Report)

18. SUPPLEMENTARY NOTES

19. KEY WORDS (Continue on reverse side if necessary and identify by block number)

Contrast Transmission	Absorption
Radiative Transfer	Visibility
Scattering	

20. ABSTRACT (Continue on reverse side if necessary and identify by block number)

A computationally efficient method called DART for simulating radiative transfer (including curvature effects) was adapted to the estimation of contrast transmission in an illuminated sky, and tested against comparable Monte Carlo simulations with a code called FLASH. The testing procedure raised several questions concerning the FLASH code, and therefore did not resolve questions concerning DART.
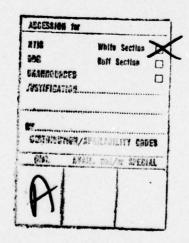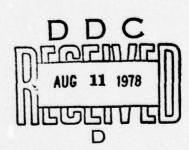
408 386

TABLE OF CONTENTS

D D C
RECEIVED
AUG 11 1978
D

iii

LIST OF SYMBOLS

A_P	Perturbed surface albedo.
A_N	Nominal surface albedo.
$_sA(z)$	Scalar albedo at altitude z, defined by the equation $_sA(z) \equiv h(z,u)/h(z,d)$.
FTT	Maximum forward-scatter optical depth for given scan and sun directions.
h	Tangent radius measured from earth's surface.
$h(z,d)$	Scalar irradiance produced by downwelling flux. This may be defined as the radiant flux from the upper hemisphere arriving at a point at altitude z.
$_kh(z,d)$	Scalar irradiance defined as the radiant flux from the upper hemisphere sky (flux from the sun is not included) arriving at a point at altitude z.
$_sh(z)$	Scalar irradiance defined as the radiant flux from the sun arriving at a point at altitude z.
$h(z,u)$	Scalar irradiance produced by upwelling flux. This may be defined as the radiant flux from the lower hemisphere arriving at a point at altitude z.
$h_k(z)$	Scalar irradiance from sky.
$h_u(z)$	Upwelling scalar irradiance from earth.
$h_s(z)$	Solar scalar irradiance.
$m_\infty(z,\theta)/m_\infty(z,0)$	Relative optical air mass.
MTAU	Multiple-scatter optical thickness.
$N(z,\theta,\phi)$	Radiance as determined from altitude z in the direction specified by zenith angle θ and azimuth ϕ.
$n(z)$	Refractive index at altitude z.

78 08 03   29

$N_q(z,\theta,\phi)$ Equilibrium radiance at altitude z with the direction of the path of sight specified by zenith angle θ and azimuth ϕ. This property is a point function of position and direction.

$\bar{N}_q(z,\theta,\phi)$ Effective equilibrium radiance for a path of sight from out of the atmosphere to altitude z in the direction specified by zenith angle θ and azimuth ϕ. This property may be defined by the equation $N_q(z,\theta,\phi) \equiv N_\infty^*(z,\theta,\phi)/\{1 - T_\infty(z,\theta)\}$. This property may also be denoted as a function of angle from light source (sun or moon) β, i.e., $\bar{N}_q(z,\beta)$.

$N_{r,A}$ Background signal from atmosphere.

$N_{r,B}$ Background signal.

$N_{r,G}$ Background signal from ground.

$N_r^*(z,\theta,\phi)$ Path radiance as determined at altitude z at the end of a path of sight of length r in the direction specified by zenith angle θ and azimuth ϕ.

P Path radiance.

$P(z)$ Pressure at altitude z.

Δr_i Refracted path length.

$s(z)$ Total volume scattering coefficient as determined at altitude z. This property may be defined by the equation $s(z) \equiv \int_{4\pi} \sigma(z,\beta)\, d\Omega$.

T_c Contrast transmission.

$T_r(z,\theta)$ Beam transmittance as determined at altitude z for a path of sight of length r at zenith angle θ. This property is independent of azimuth in atmospheres having horizontal uniformity. It is always the same for the designated path of sight or its reciprocal.

z Altitude, usually used as above ground level.

Δz Altitude increment.

β Symbol for scattering angle of flux from a light source. It is equal to the angle between the line from the source to the observer and the path of sight.

β'   Symbol for scattering angle of flux from a discrete part of the sky. It is equal to the angle between the direction specified by θ' and φ' and the path of sight.

Δ   Symbol to indicate incremental quantity and used with r and z to indicate small, discrete increments in path length r and altitude z; and with MTAU to indicate increment in optical thickness.

ζ   Symbol for radius of the earth.

θ   Symbol for zenith angle. This is usually used as one of two coordinates to specify the direction of a path of sight.

θ'   Symbol for zenith angle usually used as one of two coordinates to specify the direction of a discrete portion of the sky.

σ   Symbol for volume scattering function. Parenthetical symbols may be added; for example, β may be used to designate the scattering angle from a source. In Reference 7, the parenthetical symbols are z and β for altitude and scattering angle.

σ(z,β)/s(z)   Proportional directional volume scattering function. This may be defined by the equation $\int_{4\pi} [\sigma(z,\beta)/s(z)] \equiv 1.$

φ   Symbol for azimuth. The azimuth is the angle in the horizontal plane of the observer between a fixed point and the path of sight. The fixed point may be, for example, true north, the bearing of the sun, or the bearing of the moon. This symbol is usually used as one of two coordinates to specify the direction of a path of sight.

φ'   This symbol for azimuth is usually used as one of two coordinates to specify the direction of a discrete portion of the sky.

Ω   Symbol for solid angle. For a hemisphere $\Omega = 2\pi$ steradians; for a sphere $\Omega = 4\pi$ steradians.

SECTION 1

INTRODUCTION

This contract was aimed at adapting an existing radiative transfer-simulation computer program called DART[1-4]* for use on the Air Force Geophysics Laboratory (AFGL) computer system, and conducting exploratory calculations with existing and adapted program versions, including problems such as:

(1) Comparing computer-code results with Monte Carlo simulations and other results available in the literature that are suitable for assessing the speed and accuracy of this method.

(2) Estimating contrast transmission in an illuminated sky with particular attention to the effect of sky background radiance due to scattered sunlight, including geometries where the sun is near or below the horizon.

The adapted DART code has been delivered to AFGL, where simulations have been run and compared with Monte Carlo results.

The following paragraphs detail these efforts, including theoretical considerations, programming and debugging tasks, and generation of comparison data.

---

* Superscript numerals refer to similarly numbered items in the List of References.

SECTION 2

THEORETICAL CONSIDERATIONS

The theoretical work performed has been aimed at identifying potential generalizations and improvements of existing formulas relating to contrast-transmission calculations, especially in cases where such improvements can be implemented with the DART code.

2.1 Contrast-Transmission and Albedo Variation

Contrast transmission is defined as the ratio of apparent to inherent contrast. In Reference 5, contrast transmission is expressed mathematically for the case of a target resting on the earth and observed from an aircraft:

$$T_c = \frac{N_{r,B}}{N_{r,B} + P} \tag{1}$$

where $N_{r,B}$ is the background signal, and P is the path radiance. But in general, the target can be airborne, so that the "background" need not only be the ground. It may also be a combination of ground and atmosphere, in the case where the viewer looks generally downward at an airborne target; or it may be only atmosphere, in the case where the viewer looks generally upward at the target.

These generalizations suggest that new consideration be given to the current procedure for estimating the functional dependence of contrast transmission on surface albedo presented in Reference 5. The procedure is based upon the assumption that $N_{r,B}$ arises totally from the ground, and that only the surface albedo in the immediate vicinity of the target is changed so that only the ground signal is affected.

2

When the surface albedo changes from some nominal value, A_N, to a perturbed value, A_p, the contrast transmission changes to

$$T_c(A_p) = \frac{N_{r,B}(A_p/A_N)}{N_{r,B}(A_p/A_N) + P} \tag{2}$$

which Reference 5 shows to be equivalent to

$$T_c(A_p) = \frac{A_p T_c(A_N)}{A_N + (A_p - A_N)T_c(A_N)} \tag{3}$$

A necessary generalization of $N_{r,B}$ includes a contribution from the atmosphere, created between the ground and the target and attenuated between the target and the observer. Then

$$N_{r,B} = N_{r,G} + N_{r,A} \tag{4}$$

where G denotes ground, and A denotes atmosphere. For this case, changing the surface albedo changes the contrast transmission to

$$T_c(A_B) = \frac{N_{r,G}(A_p/A_N) + N_{r,A}}{N_{r,G}(A_p/A_N) + N_{r,A} + P} \tag{5}$$

which is equivalent to

$$T_c(A_B) = \frac{(N_{r,G}A_p + N_{r,A}A_N)T_c(A_N)}{\left[(N_{r,B} + N_{r,A})A_N + (N_{r,B}A_p + N_{r,A}A_N)T_c(A_N) - (N_{r,B} + N_{r,A})A_N T_c(A_N)\right]} \tag{6}$$

This is similar to the more special formulation, but with A_p replaced by

$$A_p' = \frac{A_p N_{r,G} + A_N N_{r,A}}{N_{r,G} + N_{r,A}} \tag{7}$$

2.2 Atmospheric Modeling

Several AFGL-sponsored reports from the Visibility Laboratory of the Scripps Institution of Oceanography were provided by AFGL to The Charles Stark Draper Laboratory, Inc., (CSDL), and were reviewed.

3

Several points of discussion were identified, all relating to formulas that are conveniently summarized with definitions of terms in Reference 6, and derivations that originate in Reference 7. The points of discussion are:

(1)   Estimation of vertical transmittance.

(2)   Computation of path length in a refracting medium.

(3)   Estimation of phase function from sky radiance.

(4)   Modeling of a clear atmosphere.

The present work suggests possible improvements in these areas because it admits a completely arbitrary multiple-constituent layered atmosphere in place of the more idealized atmospheres that have been treated previously.

2.2.1 Estimation of Vertical Transmittance

Equation 2.2 of Reference 6 gives the following equation to be solved iteratively for the vertical transmittance $T_\infty(z,0°)$:

$$\frac{N^*_\infty(z,\theta,\phi)}{N^*_\infty(z,\theta',\phi')} = \frac{\left[1 - T_\infty(z,0°)^{m_\infty(z/\theta)/m_\infty(z,0°)}\right]}{\left[1 - T_\infty(z,0°)^{m_\infty(z,\theta')/m_\infty(z,0°)}\right]} \tag{8}$$

where $N^*_\infty(z,\theta,\phi)$ is the path radiance from ∞ to altitude (z) at azimuth (ϕ) and zenith (θ), and m is the air mass. This equation invites two theoretical criticisms:

(1)   The equation is derived under the assumption of equal effective equilibrium radiances

$$\bar{N}_q(z,\theta,\phi) = \bar{N}_q(z,\theta',\phi') \tag{9}$$

for equal scattering angles

$$\beta = \beta' \tag{10}$$

Experimental data in Reference 7 supports such an assumption, but the experimental conditions may be somewhat special in that the sun is fairly near zenith (25°), and the optical depths are fairly large (paths from 1,000 to 20,000 feet). The first condition makes the radiance N^*_∞ fairly uniform in ϕ, and the second makes it fairly uniform in θ. But if the

4

sun were low in the sky and the detector were at high
altitude, the N_∞^* would not be so uniform, with the result
that $\bar{N}_q$ would depend on θ and ϕ, and not just β.

(2)   The equation is based on the model

$$T_\infty(z,\theta) = T_\infty(z,0°)^{m_\infty(z,\theta)/m_\infty(z,0°)} \tag{11}$$

The implied scaling is not as simple as it looks, since
the curved multiconstituent layered atmosphere may require
a detailed calculation to evaluate $m_\infty(z,\theta)$. For θ near 90°,
it does not vary simply as sec θ.

2.2.2 Computation of Path Length in a Refracting Medium

Equation 2.5 of Reference 6 estimates refracted path length as

$$\Delta r_i = \left\{ 1 - \left[\frac{n(0)}{n(z_i)} \frac{\zeta}{(\zeta + z_i)} \sin \theta \right]^2 \right\}^{-1/2} \Delta z \tag{12}$$

where $n(z_i)$ is the refractive index at altitude z_i, ζ is the earth
radius, and Δz is the attitude increment. This equation has at least
two defects:

(1)   The refractive index at the ground, $n(0)$, is involved.
       This should not be, since insertion of a temperature
       aberration at ground can change $n(0)$ arbitrarily, and
       hence change the estimate of Δr_i, even though Δz is
       far above ground. Clearly, Δr_i ought to depend not on
       $n(0)$, but only on $n(z_i)$ and $n(z_i + \Delta z)$.

(2)   The earth radius is involved, where actually one might
       expect the tangent radius of the scan.

A solution to the problem of estimating path length in a refracting
medium can be provided, following the work of Hayes and Robel.[8]
They note that throughout a scan path, the quantity $[n(z)(\zeta + z) \sin \theta]$
is a constant, the tangent radius, h, projected from $z = \infty$. It then
follows from an analysis of right triangles having sides $\zeta + z$, r,
and $h/n(z)$ that

$$\Delta r = \left\{ (\zeta + z + \Delta z)^2 - \left[\frac{h}{n(z + \Delta z)} \right]^2 \right\}^{1/2} - \left\{ (\zeta + z)^2 - \left[\frac{h}{n(z)} \right]^2 \right\}^{1/2} \tag{13}$$

5

2.2.3 Estimation of Phase Function from Sky Radiance

Reference 6, Eq. 2.7 proposes a basis for phase function estimation, namely

$$\frac{\sigma(z,\beta)}{s(z)} = \frac{\left[\bar{N}_q(z,\theta,\phi) - {_k}\frac{h(z,d)+h(z,u)}{4\pi}\right]}{\left[{_s}h(\infty)T_\infty(z,\theta_s)\right]}$$ (14)

where

σ is the volume scattering function.

s is the normalization factor ($s = \int \sigma \, d\Omega$).

h is radiance arriving at a point, left subscript k means from atmosphere, left subscript s means from sun.

$\bar{N}_q$ is effective equilibrium radiance.

The text notes that the formula leads to inconsistencies in application. This is to be expected for the following reasons:

(1) Absorption has not been accounted for. The right side of the equation differs from the left side by at least a factor of scattering efficiency.

(2) The second term on the right side of the equation is present to cancel the diffuse term in $\bar{N}_q$. The cancellation requires equality between

$${_k}\frac{h(z,d)+h(z,u)}{4\pi}$$

and

$$\frac{\int_{z'=z}^{\infty} \int_{4\pi} N(z',\theta',\phi')\sigma(z',\beta') \, d\Omega \, T(z',\theta) \, dz'}{1 - T_\infty(z,\theta)}$$

The required cancellation is an elaboration on a simpler one proposed in Reference 7, where the second term has no z averaging, and is just

$$\int_{4\pi} N(z,\theta',\phi') \frac{\sigma(z,\beta')}{s(z)} \, d\Omega$$

6

This equality has been proposed in Reference 7 again because of the experimental data reported there. It may not be justified if z is at an altitude such that the remaining atmosphere is thin, or if scattering is highly anisotropic. In those cases, N and/or σ depend strongly on the angles, and the angular integral of the product $N\sigma$ is not $1/4\pi$ times the product of the individual integrals.

2.2.4 Modeling of a Clear Atmosphere

Equation 2.11 of Reference 6 provides the following approximate model for equilibrium radiance.

$$N_q(0,\beta) = s h(0) \left\{ \frac{\sigma(0,\beta)}{s(0)} + \frac{s^A}{4\pi} + \frac{\left(\frac{1 + s^A}{4\pi}\right) \int_{2\pi} \left[\frac{\sigma(0,\beta')}{s(0)} + \frac{s^A}{4\pi} \right]\left[1 - T_\infty(0,\theta') \right] d\Omega}{1 - \left(\frac{1 + s^A}{4\pi}\right) \int_{2\pi} \left[1 - T_\infty(0,\theta') \right] d\Omega} \right\}$$

(15)

The derivation is in Reference 7, and the following points should be borne in mind:

(1) Equilibrium radiance is assumed to be independent of altitude. This requires a fairly thin total optical depth to assure no substantial dimming at the bottom.

(2) Equality is assumed between

$$\frac{h_k(z) + h_u(z)}{4\pi}$$

and

$$\int N(z,\theta',\phi') \frac{\sigma(z,\beta')}{s(z)} \ d\Omega$$

This requires fairly isotropic scattering and/or fairly thick optical depth.

(3)   "Albedo", $_sA$ in Reference 6, is defined in Reference 7
       as the radiance ratio

$$A_s = \frac{h_u(z)}{h_s(z) + h_k(z)} \tag{16}$$

       instead of the usual flux ratio. This means that A_s is
       not strictly a surface property, but depends on sun angle,
       optical depth, and altitude. It is therefore difficult
       to argue that the $N_q(0,\beta)$ that is a function of A_s is not
       also a function of these other variables.

As an alternative, a computer code such as DART could provide a
more consistent model of a clear atmosphere. Furthermore, it would
apply for a turbid atmosphere also, and would be almost as convenient
as the more limited analytical model.

8

SECTION 3

PROGRAMMING TASKS AND DEBUGGING

The programming and debugging tasks centered on converting the IBM Fortran code to CDC Fortran, making comparative runs in the two languages using the AFGL and CSDL computing facilities, and, most particularly, restructuring the code in a format suited to the AFGL application, including contrast transmission. A detailed description of these areas follows.

The IBM-CDC translation problem has been largely automated so that it will always be a straightforward matter to provide a most up-to-date code version for the AFGL facility. This has been done numerous times during the course of restructuring, as program changes were made, and comparative runs have verified the success of the procedure.

The program restructuring consisted of breaking the code into a number of small subroutines. The new program structuring offers considerable flexibility. It allows efficient processing for various kinds of production runs that involve only some of the subroutines. Also, it allows interfacing with a driver code that inverts measured scattering data for atmospheric parameters. The latter type of application is not specifically required in the present contract, but has in the past and may in the future be of interest to the Air Force. Documentation relevant to this type of problem was generated by CSDL under NASA sponsorship, and has been provided to AFGL.[9,10]

The calculation of contrast transmission is a problem not previously treated by the DART code, and it requires a number of program changes and improvements. These are listed and briefly described.

    (1)   Contrast-transmission calculations require treatment of an airborne detector. The DART code had previously been used for satellite-borne detectors (limb-scan problems), and earth-based detectors (twilight-simulation problems). Treatment

9

of an airborne detector required an interpolation routine
to handle the situation where the detector falls in the
interior of one of the multiple-scattering layers. Linear
interpolation was found inadequate, so a new interpolation
was developed from the following observations. The sensed
radiance contribution from a path of multiple-scattering
optical depth ΔMTAU up to the detector is generally propor-
tional to an integral of an exponential representing the
total damping. Neglecting damping along the input direction,
the integral is just

$$\int_0^{\Delta MTAU} \exp(-MTAU) \, dMTAU = 1 - \exp(-\Delta MTAU) \qquad (17)$$

If we have a full path of depth $\Delta MTAU_{full}$ and a portion of
depth $\Delta MTAU_{portion}$, the ratio of their radiance contributions
is approximately

$$\frac{\left[1 - \exp\left(-\Delta MTAU_{portion}\right)\right]}{\left[1 - \exp\left(-\Delta MTAU_{full}\right)\right]}$$

This ratio provides a factor that accomplishes the desired
interpolation. It reduces to the original linear inter-
polation for small ΔMTAUs, but otherwise provides a some-
what larger and more realistic radiance.

(2) Calculation of contrast transmission requires separation of
background and path radiances. This was accomplished by
introducing the concept of a "target" defining the end of the
path and the beginning of the background. The total radiance
and the contribution of the path alone were computed, with
the background being obtained as the difference. This
approach requires calculation of the singly scattered path
radiance, the prior estimate of multiply scattered path
radiance, and the posterior estimate of multiply scattered
path radiance (see Reference 4). All computations of
single-scatter radiance and prior-estimate radiance
depend on sums of incremental combinations for small
atmospheric layers that are accumulated along the scan

10

direction moving away from the detector. The sums newly
required for the contrast-transmission case are accumulated
in the usual way, but terminated and saved as soon as
the "target" is reached. All posterior estimates of
multiply-scattered radiance are constructed according
to Bayes' rule.[2] Those newly required for the contrast-
transmission case are constructed as usual, but using the
appropriate prior estimate.

(3)   The DART code calculates single scattering exactly, and
uses the result to replace the singly scattered portion
of the more approximate multiple scattering. This
replacement requires a suitable estimate of the portion
of multiple scattering to be deleted. A previously
existing estimation routine, which was based on the
optical depth in the direction of stream propagation,
was found to be inadequate because of the wide variety
of optical depths and scan directions encountered in
contrast-transmission problems. The code was changed
so that, instead, deletion was based on optical depth
in the actual sun and scan directions. The deletion
factor used represents the probability that at least
one forward scatter occurs on a path having a particular
scan direction and sun direction. It is evaluated as
1 minus the probability of no forward scatters. The
latter probability is estimated as exp(-FTT), where FTT
is the maximal forward-scatter optical depth that occurs
for a path having the particular scan direction and sun
direction.

(4)   Production runs will generally require variation of many
variables, and for efficiency it is desirable to allow
such variation within a single run of the code. The DART
code was already equipped to handle multiple polar view
angles or multiple sun positions. In addition, provision
was made for multiple targets. This provision will be
useful in the context of airborne targets because it
will facilitate answering questions such as "for a given
problem geometry, how far away can a target be detected?"

11

SECTION 4

COMPARISON WITH MONTE CARLO

Radiances and contrast transmissions have been calculated by
the DART code and FLASH Monte Carlo code.[11-14] This section details
these comparisons.

4.1 Cases Compared

The problems use a unit irradiance beam of 5,500 angstroms wave-
length incident on a 1968 standard atmosphere,[15] and a selected set
of geometries. Combinations of solar zenith angles (20, 60, and 85°),
solar azimuth angles (0, 90, and 180°), and detector polar view angles
(97, 100, 110, 120, 140, 160, and 175°) are included. Figure 1 shows
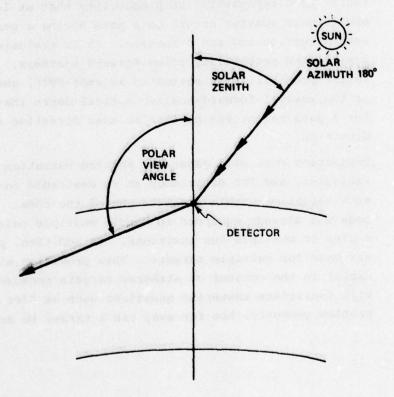the problem geometry. The detector altitude is 12,000 feet.

Figure 1.   Problem geometry.

12

4.2   Atmospheric Models and Differences

Each code uses a layered model extending from the earth's surface to an altitude of 50 kilometers. The FLASH model uses 24 layers of graduated thickness beginning with a 0.5-kilometer thickness for the bottom layer, and ending with a 5-kilometer thickness at the top. The DART model uses fifty 1-kilometer-thick layers.

Reference 15 provides the basic atmospheric model (except for the phase function) for both codes, but the raw data presented requires translation to inputs in the proper formats for the two codes. Program requirements differ, and the translations were done by different individuals at AFGL and CSDL using different conversion codes. The net result is some difference in optical thicknesses going into the two codes (see Table 1).

Table 1. Optical depths.

	FLASH Input	DART Input	Difference (%)
Total	0.3677	0.3593	2.3
Absorption	0.0355	0.0293	17.0

Although the absorption optical depths are significantly different, it is expected that this difference will have little effect, since the detector is at low altitude where the optical depth from the detector to the surface is only about 1-percent absorbing.

The single-scattering phase function was generated in each case by the same MIE code; however, the AFGL values were computed much earlier, and information about the particle-size-integration step was not retained from those computations. Therefore, 100 integration steps were chosen to produce the DART inputs. Small differences in the phase functions resulted, such as the typical values given in Table 2.

Both codes used a Lambertian reflecting surface at an earth radius of 6,378.383 kilometers, with 0.18 albedo. The detector altitude was read in as 3.7 kilometers in the DART code, and 3.6576 kilometers in the FLASH code.

13

Table 2. Phase-function values (steradians^{-1}).

Phase Function	FLASH Input	DART Input	Difference (%)
At 0°	6.59	6.52	1.1
At 20°	0.472	0.466	1.3
At 40°	0.0165	0.0167	1.2
At 80°	0.0348	0.0336	3.3
At 120°	0.0131	0.0132	1.0
At 140°	0.0136	0.0138	1.5
At 180°	0.0360	0.0361	0.3

4.3 Single-Scattering Results

Both codes do exact single-scattering calculations, although they use different methods. Tables 3 through 5 compare single-scattering calculations for the path radiance (for unit irradiance input). Since the calculations are supposed to be exact, one might expect agreement in the tables to within the differences of the input models, i.e., a few percent. In fact, the differences are larger than this. Figure 2 illustrates typical differences. For the two smaller zenith angles, differences are compatible with the input model differences; however, for an 85° zenith, where curvature becomes important, there is considerable divergence.

Table 3. Single-scatter path radiance at 0° azimuth (unit irradiance input, 5,500 angstroms, 12,000-foot altitude).

Polar View Angle (degrees)	20° Zenith		60° Zenith		85° Zenith	
	FLASH	DART	FLASH	DART	FLASH	DART
97	0.0260	0.0249	0.0915	0.0914	0.0603	0.0748
100	0.0201	0.0189	0.0672	0.0669	0.0401	0.0496
110	0.0102	0.00971	0.0285	0.0280	0.0142	0.0178
120	0.00663	0.00635	0.0143	0.0142	0.00638	0.00817
140	0.00443	0.00442	0.00529	0.00542	0.00190	0.00252
160	0.00449	0.00463	0.00309	0.00331	0.000831	0.00113
175	0.00549	0.00575	0.00275	0.00301	0.000555	0.000776

14

Table 4. Single-scatter path radiance at 90° azimuth (unit irradiance input, 5,500 angstroms, 12,000-foot altitude).

Polar View Angle (degrees)	20° Zenith		60° Zenith		85° Zenith	
	FLASH	DART	FLASH	DART	FLASH	DART
97	0.0178	0.0173	0.0151	0.0152	0.00313	0.00388
100	0.0144	0.0137	0.0122	0.0121	0.00245	0.00303
110	0.00847	0.00811	0.00727	0.00713	0.00142	0.00176
120	0.00635	0.00609	0.00516	0.00515	0.00101	0.00128
140	0.00512	0.00512	0.00347	0.00362	0.000674	0.000893
160	0.00551	0.00561	0.00296	0.00317	0.000558	0.000760
175	0.00600	0.00632	0.00282	0.00308	0.000520	0.000727

Table 5. Single-scatter path radiance at 180° azimuth (unit irradiance input, 5,500 angstroms, 12,000-foot altitude).

| Polar View Angle (degrees)	20° Zenith		60° Zenith		85° Zenith	
	FLASH	DART	FLASH	DART	FLASH	DART
97	0.0170	0.0163	0.0230	0.0226	0.00584	0.00710
100	0.0142	0.0134	0.0198	0.0194	0.00444	0.00533
110	0.00956	0.00895	0.0135	0.0131	0.00234	0.00286
120	0.00783	0.00745	0.0112	0.0111	0.00148	0.00181
140	0.00772	0.00767	0.00622	0.00641	0.000752	0.000964
160	0.00807	0.00831	0.00363	0.00388	0.000522	0.000701
175	0.00640	0.00677	0.00295	0.00319	0.000507	0.000691

15
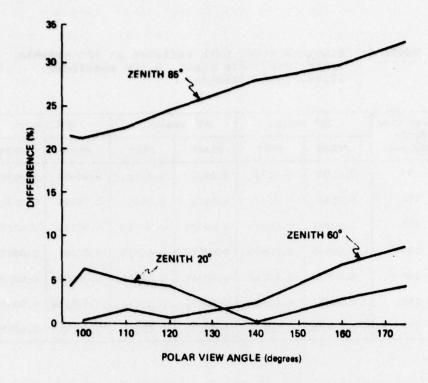
Figure 2. Single-scatter path radiance differences
between FLASH and DART (0° azimuth,
12,000-foot altitude, unit irradiance
input, 5,500 angstroms).

The dynamic range of the single-scatter path radiances over the
geometries considered is more than two orders of magnitude, and the
fact that the two codes track each other to within about 25 percent
over this range implies that there are no gross modeling errors.
However, the marked divergence at large zenith implies a modeling
difference that has not been positively identified. Aside from coin-
cidence, it is expected that if calculations of total scattering by
the two codes are to agree, the agreement ought to begin with single
scattering. Hence, agreement in multiple scattering between the two
codes in the 85° zenith case is not to be expected.

4.4 Multiple-Scattering and Contrast-Transmission Results

Tables 6 through 14 list the multiple-scattering path radiances and surface radiances for unit irradiance input, and the contrast transmissions. Tables 15 through 18 show some variations of results that were obtained by varying Monte Carlo input parameters. The following observations are made:

(1) The path radiances with multiple scattering follow the same qualitative relationship as the single-scatter values. However, in multiple scattering the differences are more pronounced. There is an increase in path radiance difference with increasing polar view angle.

(2) The FLASH multiple-scatter path radiances for a 175° polar view angle show an azimuthal dependence which is not expected. Clearly, a polar view angle of 175° is looking nearly straight downward, so there ought to be little azimuthal dependence, and indeed, little is found in single scattering. The results shown cannot be explained on the basis of phase function or extinction differences. An attempt was made to relate them to the choice of Monte Carlo input parameters, as detailed in Table 15. The results were indeed found to be sensitive to those parameters, but the problems noted were not removed, only changed. Figure 3 shows the multiple-scatter dependence for the three zenith angles considered.

(3) Surface radiances generally track the behavior of the path radiances. At the 175° polar view angle, FLASH shows a pronounced azimuth dependence even for a Lambertian surface. This was in some instances made worse by the change of input parameters that served to improve the azimuth dependence of 175° path radiances.

(4) Agreement between the contrast-transmissions (which was the chief goal of this research) is good for zenith angles of 20 and 60°. At 85°, contrast-transmission differences are excessively large. Figure 4 shows a plot of percentage difference in contrast transmissions for 90° azimuth.

17

Table 6. Radiances and contrast transmissions for 20° zenith and 0° azimuth (unit irradiance input, 5,500 angstroms, 12,000-foot altitude).

Polar View Angle (degrees)	Path Radiance		Surface Radiance		Contrast Transmission	
	FLASH	DART	FLASH	DART	FLASH	DART
97	0.0773	0.0757	0.00810	0.00884	0.0949	0.105
100	0.0649	0.0610	0.0142	0.0141	0.179	0.188
110	0.0367	0.0336	0.0259	0.0237	0.414	0.413
120	0.0267	0.0222	0.0315	0.0279	0.541	0.557
140	0.0181	0.0136	0.0376	0.0315	0.675	0.699
160	0.0160	0.0113	0.0390	0.0327	0.709	0.743
175	0.0199	0.0118	0.0557	0.0330	0.737	0.737

Table 7. Radiances and contrast transmissions for 20° zenith and 90° azimuth (unit irradiance input, 5,500 angstroms, 12,000-foot altitude).

Polar View Angle (degrees)	Path Radiance		Surface Radiance		Contrast Transmission	
	FLASH	DART	FLASH	DART	FLASH	DART
97	0.0638	0.0658	0.00803	0.00880	0.112	0.117
100	0.0522	0.0538	0.0139	0.0140	0.210	0.206
110	0.0340	0.0310	0.0262	0.0236	0.435	0.432
120	0.0251	0.0213	0.0322	0.0278	0.562	0.566
140	0.0181	0.0140	0.0374	0.0314	0.673	0.691
160	0.0169	0.0122	0.0389	0.0326	0.697	0.728
175	0.0158	0.0124	0.0376	0.0330	0.704	0.727

Table 8. Radiances and contrast transmissions for 20° zenith and 180° azimuth (unit irradiance input, 5,500 angstroms, 12,000-foot altitude).

Polar View Angle (degrees)	Path Radiance		Surface Radiance		Contrast Transmission	
	FLASH	DART	FLASH	DART	FLASH	DART
97	0.0623	0.0618	0.00808	0.00867	0.115	0.123
100	0.0505	0.0511	0.0139	0.0139	0.216	0.213
110	0.0344	0.0307	0.0263	0.0234	0.433	0.433
120	0.0267	0.0220	0.0329	0.0277	0.552	0.557
140	0.0207	0.0163	0.0375	0.0313	0.644	0.657
160	0.0189	0.0148	0.0399	0.0326	0.679	0.688
175	0.0158	0.0128	0.0350	0.0330	0.689	0.721

Table 9. Radiances and contrast transmissions for 60° zenith and 0° azimuth (unit irradiance input, 5,500 angstroms, 12,000-foot altitude).

Polar View Angle (degrees)	Path Radiance		Surface Radiance		Contrast Transmission	
	FLASH	DART	FLASH	DART	FLASH	DART
97	0.160	0.147	0.00399	0.00407	0.0238	0.0269
100	0.126	0.112	0.00675	0.00648	0.0509	0.0546
110	0.0582	0.0519	0.0122	0.0109	0.174	0.174
120	0.0347	0.0297	0.0149	0.0129	0.301	0.307
140	0.0153	0.0142	0.0181	0.0146	0.542	0.506
160	0.0110	0.00963	0.0198	0.0151	0.644	0.610
175	0.0184	0.00861	0.0538	0.0151	0.745	0.637

Table 10.   Radiances and contrast transmissions for 60° zenith
            and 90° azimuth (unit irradiance input, 5,500 angstroms,
            12,000-foot altitude).

Polar View Angle (degrees)	Path Radiance		Surface Radiance		Contrast Transmission	
	FLASH	DART	FLASH	DART	FLASH	DART
97	0.0503	0.0531	0.00377	0.00399	0.0698	0.0699
100	0.0404	0.0443	0.00659	0.00636	0.140	0.125
110	0.0256	0.0271	0.0128	0.0108	0.333	0.284
120	0.0180	0.0191	0.0152	0.0127	0.458	0.400
140	0.0114	0.0122	0.0172	0.0145	0.601	0.543
160	0.00939	0.00962	0.0193	0.0151	0.673	0.612
175	0.00726	0.00900	0.0150	0.0153	0.674	0.630

Table 11.   Radiances and contrast transmissions for 60° zenith
            and 180° azimuth (unit irradiance input, 5,500 angstroms,
            12,000-foot altitude).

Polar View Angle (degrees)	Path Radiance		Surface Radiance		Contrast Transmission	
	FLASH	DART	FLASH	DART	FLASH	DART
97	0.0609	0.0539	0.00374	0.00378	0.0579	0.0656
100	0.0521	0.0462	0.00627	0.00607	0.107	0.116
110	0.0339	0.0301	0.0123	0.0104	0.265	0.256
120	0.0237	0.0232	0.0144	0.0124	0.378	0.347
140	0.0150	0.0140	0.0181	0.0141	0.547	0.502
160	0.0109	0.00967	0.0186	0.0147	0.631	0.605
175	0.00789	0.00865	0.0144	0.0150	0.646	0.635

Table 12.   Radiances and contrast transmissions for 85° zenith
and 0° azimuth (unit irradiance input, 5,500 angstroms,
12,000-foot altitude).

Polar View Angle (degrees)	Path Radiance		Surface Radiance		Contrast Transmission	
	FLASH	DART	FLASH	DART	FLASH	DART
97	0.0894	0.1257	0.000389	0.000760	0.00433	0.00602
100	0.0645	0.0955	0.000626	0.00126	0.00961	0.0131
110	0.0252	0.0495	0.00113	0.00242	0.0427	0.0466
120	0.0124	0.0301	0.00147	0.00315	0.106	0.0947
140	0.00469	0.0132	0.00164	0.00393	0.259	0.229
160	0.00426	0.00853	0.00172	0.00404	0.287	0.321
175	0.00519	0.00730	0.00527	0.00394	0.504	0.350

Table 13.   Radiances and contrast transmissions for 85° zenith
and 90° azimuth (unit irradiance input, 5,500 angstroms,
12,000-foot altitude).

Polar View Angle (degrees)	Path Radiance		Surface Radiance		Contrast Transmission	
	FLASH	DART	FLASH	DART	FLASH	DART
97	0.0116	0.0324	0.000357	0.000753	0.0299	0.0227
100	0.00956	0.0290	0.000600	0.00125	0.0590	0.0412
110	0.00564	0.0207	0.00132	0.00234	0.190	0.101
120	0.00376	0.0159	0.00145	0.00301	0.278	0.159
140	0.00224	0.0106	0.00163	0.00379	0.421	0.263
160	0.00168	0.00825	0.00185	0.00408	0.524	0.331
175	0.00106	0.00763	0.00108	0.00416	0.505	0.353

21

Table 14. Radiances and contrast transmissions for 85° zenith and 180° azimuth (unit irradiance input, 5,500 angstroms, 12,000-foot altitude).

Polar View Angle (degrees)	Path Radiance		Surface Radiance		Contrast Transmission	
	FLASH	DART	FLASH	DART	FLASH	DART
97	0.0155	0.0312	0.000313	0.000634	0.0199	0.0199
100	0.0121	0.0274	0.000582	0.00106	0.0458	0.0372
110	0.00744	0.0193	0.000920	0.00204	0.110	0.0956
120	0.00384	0.0147	0.00118	0.00267	0.236	0.153
140	0.00245	0.00968	0.00216	0.00341	0.469	0.260
160	0.00183	0.00743	0.00180	0.00368	0.497	0.331
175	0.00130	0.00706	0.00127	0.00385	0.495	0.353

Table 15. Monte Carlo control parameters.

	Initial Value	Modified Value
Number of Photons	200/view direction	1000/view direction
SMVAL (prevents division by zero)	10^{-4}	10^{-6}
DELTA (moves collisions away from layer boundaries)	0.05 km	0.0005 km
EPSILON (convergence criterion for defining refracted path back to sun)	10^{-4} rad	10^{-5} rad

Table 16. Modifications for Tables 6, 7, and 8: radiances and contrast transmissions for 20° solar zenith angle.

Azimuth (degrees)	Polar View Angle (degrees)	Path Radiance		Surface Radiance		Contrast Transmission	
		FLASH	DART	FLASH	DART	FLASH	DART
0	160	0.0166	0.0113	0.0445	0.0327	0.728	0.743
	175	0.0172	0.0118	0.0482	0.0330	0.737	0.737
90	160	0.0163	0.0122	0.0382	0.0326	0.701	0.728
	175	0.0160	0.0124	0.0383	0.0330	0.705	0.727
180	160	0.0178	0.0148	0.0357	0.0326	0.667	0.688
	175	0.0158	0.0128	0.0357	0.0330	0.693	0.721

Table 17. Modifications for Tables 9, 10, and 11: radiances and contrast transmission for 60° solar zenith angle.

Azimuth (degrees)	Polar View Angle (degrees)	Path Radiance		Surface Radiance		Contrast Transmission	
		FLASH	DART	FLASH	DART	FLASH	DART
0	160	0.0113	0.00963	0.0233	0.0151	0.673	0.610
	175	0.0112	0.00861	0.0268	0.0151	0.705	0.637
90	160	0.00928	0.00962	0.0171	0.0151	0.648	0.612
	175	0.00853	0.00900	0.0165	0.0153	0.659	0.630
180	160	0.00884	0.00967	0.0156	0.0147	0.638	0.605
	175	0.00776	0.00865	0.0150	0.0150	0.659	0.635

Table 18. Modifications for Tables 12, 13, and 14: radiances and contrast transmissions for 85° solar zenith angle.

Azimuth (degrees)	Polar View Angle (degrees)	Path Radiance		Surface Radiance		Contrast Transmission	
		FLASH	DART	FLASH	DART	FLASH	DART
0	160	0.00266	0.00853	0.00214	0.00404	0.446	0.321
	175	0.00215	0.00730	0.00250	0.00394	0.538	0.350
90	160	0.00168	0.00825	0.00171	0.00408	0.504	0.331
	175	0.00154	0.00763	0.00154	0.00416	0.500	0.353
180	160	0.00148	0.00743	0.00154	0.00368	0.510	0.331
	175	0.00138	0.00706	0.00150	0.00385	0.521	0.353
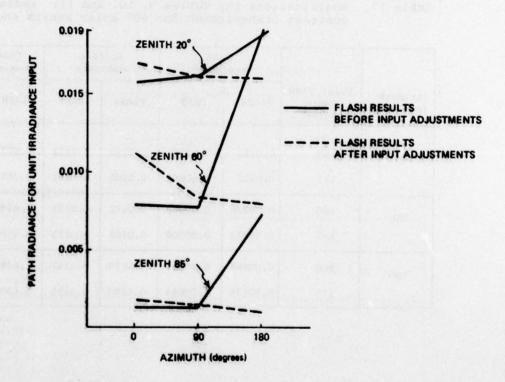
Figure 3. Azimuthal dependence of FLASH path radiance at 175° polar view angle.
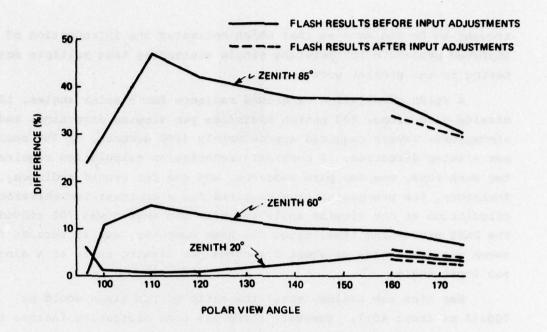
Figure 4. Percent difference between DART and FLASH contrast transmissions for 90° azimuth.

4.5 _Discussion_

At large zenith, there are substantial disagreements between the two codes that exceed expectations based upon input model differences. This disagreement is unexpected for the single-scattering calculations, and any further attempts to compare the two codes for this kind of problem should begin by focusing on single-scattering differences. The usual procedure for resolving these differences should be followed, i.e., simpler input models whose differences are as small as possible should be run, beginning with a Rayleigh atmosphere.

Both codes present areas for further investigation. The FLASH code clearly has a problem with viewing angles that are near straight down. This difficulty may be a smooth function of polar view angle so that errors of diminishing size are accrued for diminishing polar view angles. For non-Rayleigh scattering, the DART code appears to differ from other codes at or near exact forward or back scattering.[16] This phenomenon may be due mainly to the fact that DART picks up details of the phase function exactly in single scattering, whereas other methods may not. Also, the older results[16] appear generally to be bright for upward and downward scan directions. This phenomenon is

25

thought to be the same as that which motivated the introduction of an improved procedure for deleting single scattering from multiple scattering in the present work.

A FLASH calculation of ground radiance for 9 solar angles, 12 viewing directions, 800 photon histories per viewing direction, and 24 atmospheric layers required approximately 4200 seconds, or 350 seconds per viewing direction. A contrast-transmission calculation requires two such runs, one for path radiance, and one for ground radiance. Therefore, the processing time required for a contrast-transmission calculation at one viewing angle for nine sun angles was 700 seconds. The DART processing time, using the same computer, was 15 seconds for seven viewing angles or about 2 seconds per viewing angle at a single sun input angle.

For nine sun angles, then, the ratio of run times would be 700:18 or about 40:1. However, there are some mitigating factors that must be considered. First, the FLASH results showed a variance of about 3 percent, so that if one reduced the number of photon histories by a factor of 4, the run-time ratio would be reduced to 10:1 for a degradation of accuracy to 6 percent. This is still a reasonable number for these calculations. Second, the FLASH runs could have incorporated two additional ground albedo values at a very slight cost in execution time, thereby reducing the run-time ratio to 3:1. The DART code was run using a 50-layer atmosphere, while FLASH used 24 layers. In FLASH, the execution time is nearly linearly proportional to the number of layers. In DART, the run-time relationship to number of layers has not been determined, but it is expected to be less than linear. That is, a halving of the layer number is not expected to cause a halving of run time because the multiple-scattering calculations, which consume most of the run time, are not affected by the total number of layers, but rather by the number of multiple-scattering groups into which these layers are combined.

26

LIST OF REFERENCES

1. Whitney, C. K., R. E. Var, and C. R. Gray, <u>Research Into Radiative Transfer Modeling and Applications</u>, AFCRL-TR-73-0420, July 1973.

2. Whitney, C. K., "Extending Radiative Transfer Models by Use of Bayes' Rule", <u>Journal of Atmospheric Sciences</u>, Vol. 34, May 1977, pp. 766-772.

3. Whitney, C. K., "Implications of a Quadratic Stream Definition In Radiative Transfer Theory", <u>Journal of the Atmospheric Sciences</u>, Vol. 29, No. 8, November 1972, pp. 1520-1530.

4. Whitney, C. K., "Efficient Stream Distributions in Radiative Transfer Theory", <u>Journal of Quantitative Spectroscopy and Radiative Transfer</u>, Vol. 14, 1974, pp. 591-611.

5. Shettle, E., <u>Calculations of the Optical Reduction in the Visible and Near IR Through Clear and Hazy Atmospheres</u>, AFCRL Environmental Consultation Service RCS No. 3-101, October 1973.

6. Duntly, S. Q., R. W. Johnson, and J. I. Gordon, <u>Airborne Measurements of the Optical Atmospheric Properties, Summary and Review II</u>, AFCRL-TR-75-0457, September 1975.

7. Gordon, J. I., "Model for a Clear Atmosphere", <u>Journal of the Optical Society of America</u>, Vol. 59, January 1969, pp. 14-18.

8. Hayes, P. B., and R. D. Robel, "Stellar Spectra and Atmospheric Composition", <u>Journal of the Atmospheric Sciences</u>, Vol. 25, November 1968, pp. 1141-1153.

9. Malchow, H. L., C. K. Whitney, D. P. Latimer, and C. R. Gray, <u>User Guide for Sunlit Limb Inversion Code (SLIC)</u>, Charles Stark Draper Laboratory Report R-1032, January 1977.

10. Malchow, H. L., C. K. Whitney, D. P. Latimer, and C. R. Gray, <u>Program Guide for Sunlit Limb Inversion Code (SLIC)</u>, Charles Stark Draper Laboratory Report R-1033, January 1977.

LIST OR REFERENCES (Cont.)

11. Blattner, W., D. Collins, and M. Wells, <u>Monte Carlo Calculations in Spherical-Shell Atmospheres</u>, AFCRL-71-0382, June 1971.

12. Collins, D., and M. Wells, <u>Flash, a Monte Carlo Procedure for Use in Calculating Light Scattering in a Spherical Shell Atmosphere</u>, AFCRL-70-0206, January 1970.

13. Collins, D. G., et al., "Backward Monte Carlo Calculations of the Polarization Characteristics of the Radiation Emerging from Spherical-Shell Atmospheres", <u>Applied Optics</u>, Vol. 11, 1972, pp. 2684-2696.

14. Blattner, W. G., et al., "Monte Carlo Studies of the Sky Radiation at Twilight", <u>Applied Optics</u>, Vol. 13, 1974, pp. 534-547.

15. Elterman, L., <u>UV, Visible, and IR Attenuation for Altitudes to 50 km, 1968</u>, AFCRL-68-0153, April 1968.

16. Lenoble, J., ed., <u>Standard Procedures to Compute Radiative Transfer in a Scattering Atmosphere</u>, IAMAP Radiation Commission, July 1977, pp. 97ff.